

# ChemComm

Accepted Manuscript



This is an *Accepted Manuscript*, which has been through the Royal Society of Chemistry peer review process and has been accepted for publication.

*Accepted Manuscripts* are published online shortly after acceptance, before technical editing, formatting and proof reading. Using this free service, authors can make their results available to the community, in citable form, before we publish the edited article. We will replace this *Accepted Manuscript* with the edited and formatted *Advance Article* as soon as it is available.

You can find more information about *Accepted Manuscripts* in the [Information for Authors](#).

Please note that technical editing may introduce minor changes to the text and/or graphics, which may alter content. The journal's standard [Terms & Conditions](#) and the [Ethical guidelines](#) still apply. In no event shall the Royal Society of Chemistry be held responsible for any errors or omissions in this *Accepted Manuscript* or any consequences arising from the use of any information it contains.



Journal Name

COMMUNICATION

Received 00th January 20xx,  
Accepted 00th January 20xx

DOI: 10.1039/x0xx00000x

www.rsc.org/

## Metal-free boron-doped graphene for selective electroreduction of carbon dioxide to formic acid / formate

Narayanan Sreekanth<sup>a†</sup>, Mohammed Nazrulla Azeezulla<sup>b†</sup>, Thazhe Veettil Vineesh<sup>a</sup>, Krishnamurthy Sailaja<sup>b\*</sup>, Kanala Lakshminarasimha Phani<sup>a\*</sup>

**Herein we report the electrocatalytic activity of boron-doped graphene for the reduction of CO<sub>2</sub>. Electrolysis takes place at low over potentials leading exclusively to formate as the product (vis-à-vis benchmark Bi catalyst). Computational studies reveal mechanistic details of CO<sub>2</sub> adsorption and subsequent conversion to formic acid/formate.**

In the past few decades, significant change in the climate is due to enormous increase in the concentration of greenhouse gases in the atmosphere. Among these gases, the content of CO<sub>2</sub> is quite high.<sup>1</sup> Converting greatly abundant CO<sub>2</sub> to next generation fuels like formic acid and methanol is attractive and thus has become the focal theme of research and development.<sup>2</sup> Electrochemical reduction of CO<sub>2</sub> to value-added chemicals using renewable energy is one approach to help address this problem as it will recycle 'spent' CO<sub>2</sub> and it provides a method to store or utilize otherwise wasted excess renewable energy from intermittent sources.<sup>3</sup>

Metal-free electrocatalysts can be next-generation, renewable materials that hold promise to be cost-effective, relative to their metal-containing counterparts.<sup>4</sup> These catalysts can be classified into four main categories, including conjugated polymers,<sup>5</sup> pyridinium derivatives,<sup>6</sup> aromatic anion radicals<sup>7</sup> and heteroatom-doped carbon materials.<sup>8</sup> Among the currently studied metal-free electrocatalysts of CO<sub>2</sub> reduction reaction (CO<sub>2</sub>RR), only the mechanism of pyridinium-based systems has been examined by computational studies.<sup>6</sup> Mechanistic insights into the catalytic performance of the

other systems are yet to be gained. In the recent times, non-metallic low cost heteroatom-doped carbon-based catalysts have shown promise as high performance catalysts replacing precious metal catalysts for electrochemical oxygen reduction reaction (ORR).<sup>9</sup> A contemporary interest is to dope carbons with multiple heteroatoms, so called co-doped -graphene and -CNTs for ORR electrocatalysis.<sup>10</sup> Heteroatom doping can endow graphene with various new or improved electrical, physicochemical, optical, and structural properties and is also expected to create catalytically active centers.<sup>11</sup>

In heterogeneous catalysis, nitrogen-doped carbon nanotubes (NCNT) were found by Meyer et al<sup>8a</sup> to function as catalyst to reduce CO<sub>2</sub> to formate in aqueous bicarbonate solutions, with its faradaic efficiency 59% and NCNT with a modification of polyethylenimine, faradaic efficiency reaching 85%. And carbon nano-fibres in ionic liquids reduce CO<sub>2</sub> to CO at lower overpotentials and higher efficiency than silver.<sup>8b</sup> Very recently, Ajayan's group has reported selective and stable CO<sub>2</sub>RR (to CO) on nitrogen-doped carbon nanotubes.<sup>8c</sup> However, it is difficult to discern the essential difference between the nitrogen-doped CNTs both groups have used that seemingly lead to different products, viz., CO and formate.

The activity of boron-doped graphene towards CO<sub>2</sub>RR remains sparsely explored or even unknown. Here, we show that boron-doped graphene (BG) catalyses electrochemical reduction of CO<sub>2</sub> to formate efficiently. It occurs under thoroughly mild conditions, and formate is the only product obtained by the direct reduction of CO<sub>2</sub>. Based on the tendency of CO<sub>2</sub> to adsorb on boron-nitride tubes,<sup>12</sup> electroreduction at boron-doped diamond electrodes,<sup>13</sup> we expect that CO<sub>2</sub> can favourably adsorb on boron-doped matrices and also undergo reduction. Motivated by these observations, we interrogated the electrocatalytic activity of metal-free BG for the reduction of CO<sub>2</sub> in aqueous 0.1 M KHCO<sub>3</sub> solutions. In what follows, both experimental and theoretical studies prove BG to be a good candidate for CO<sub>2</sub> reduction to formic acid/formate.

<sup>a</sup> Mr. Narayanan Sreekanth, Mr Thazhe Veettil Vineesh and Dr. Kanala Lakshminarasimha Phani\*, Nanoscale Electrocatalysis Group, Electrodeposits & Electrocatalysis Division, CSIR-Central Electrochemical Research Institute Karaikudi 630006 India. Fax: (+) 914565227779, 227713, E-mail: kanalaphani@yahoo.com; klnphani@cecri.res.in

<sup>b</sup> Mr Mohammed Azeezulla Nazrulla, Dr. Krishnamurthy Sailaja, Functional Materials Division, CSIR-Central Electrochemical Research Institute Karaikudi 630006 India.

† These authors contributed equally.

Electronic Supplementary Information (ESI) available: [details of any supplementary information available should be included here]. See DOI: 10.1039/x0xx00000x

We synthesized BG by heating a uniform (1:5 wt) mixture of graphene oxide (GO) and boric acid at 900°C in Ar atmosphere, (method of synthesis explained in ESI). X-ray photoelectron spectroscopy (XPS) and Raman spectroscopy confirmed boron-doping of graphene (Figure 1). XPS signals of B1s and C1s at 189.4, 190.50, 191.9 and 284.9 eV respectively show the presence of boron atom in the hexagonal graphitic plane<sup>10, 14</sup>. Based on the XPS spectra B content is estimated to be 4.1 at%. Increase of the ID/IG ratio in the Raman spectra of BG (figure 1(d)) vis-à-vis graphene oxide indicates that the defects arise due to doping<sup>10,14</sup> (materials characterization explained in ESI.)

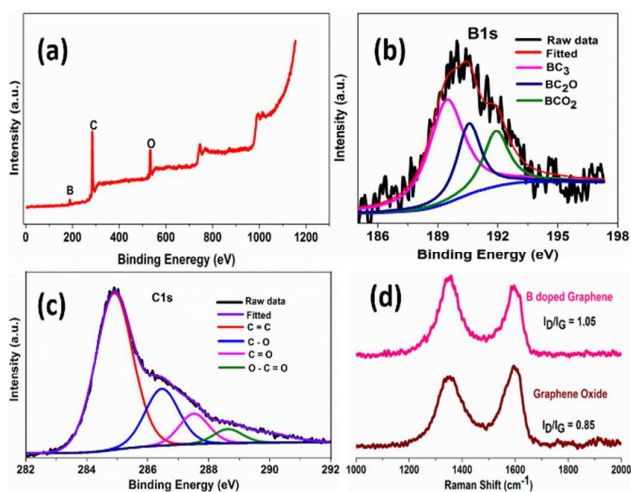
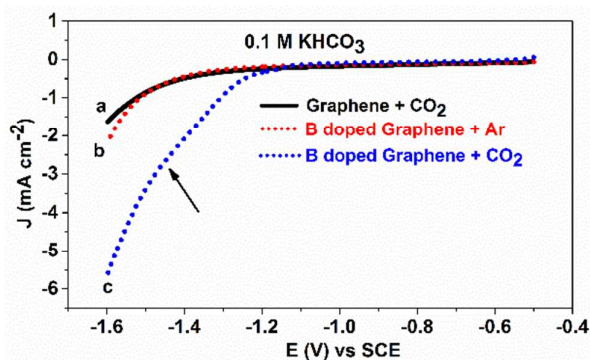


Fig. 1 (a) XPS survey spectrum of BG. High resolution XPS spectra of (b) B1s and (c) C1s. and (d) Raman spectra of GO and BG.

The electrocatalytic activity of graphene and BG were examined in Ar- saturated and CO<sub>2</sub>-saturated 0.1 M KHCO<sub>3</sub> solutions. Figure 2 shows the linear sweep voltammogram (LSV) of CO<sub>2</sub> reduction on BG and graphene acquired by sweeping the potential between -0.5 to -1.6V vs saturated calomel electrode (SCE) at a sweep rate of 0.05Vs<sup>-1</sup>. In comparing LSV of BG in CO<sub>2</sub>-free and CO<sub>2</sub>-saturated bicarbonate solutions, a clear change in the voltammogram becomes noticeable. Unlike the featureless voltammograms obtained for CO<sub>2</sub> reduction on metal electrodes in aqueous electrolytes, a current plateau is obtained at -1.4 V with a current onset at -1.1V. Further, the current keeps increasing with at least 3 times higher current obtained at -1.6 V compared to the CO<sub>2</sub>-free situation, followed by a current rise due to hydrogen evolution. But in the case of pristine graphene, no activity towards CO<sub>2</sub> reduction is observed except the onset of hydrogen evolution at much higher potentials.

We have carried out DFT calculations in order to discern the electrocatalytic activity of BG vis-à-vis graphene and further gain insights into the mechanism of CO<sub>2</sub>RR, yielding formic acid as a major product. C<sub>42</sub>H<sub>16</sub> and C<sub>41</sub>BH<sub>16</sub> structures are considered to model the cases of graphene and BG. The origin of the electrocatalytic activity of BG compared to graphene stems from the process of doping which is an efficient and effective way to tune the physicochemical properties of a material. In the present case, analysis of the frontier molecular orbitals of pristine graphene (C<sub>42</sub>H<sub>16</sub>) reveals that there is a symmetrically

distributed electron delocalization<sup>15</sup> (HOMO in ESI Figure S7b.) which is broken in BG (HOMO in Figure 3a). In addition, the presence of boron also introduces asymmetric charge and spin density distribution throughout the ground state geometry resulting in a high spin density (Figure 3b). In spin density mapping, the red colour indicates positive spin density and green colour represents negative spin density. It is clear that due to doping, spin density is distributed, *albeit* asymmetrically, throughout the system. Moreover, positive spin density on B and C atoms also suggests that both atoms are catalytically active and available for chemisorption. This makes BG an attractive metal-free candidate for

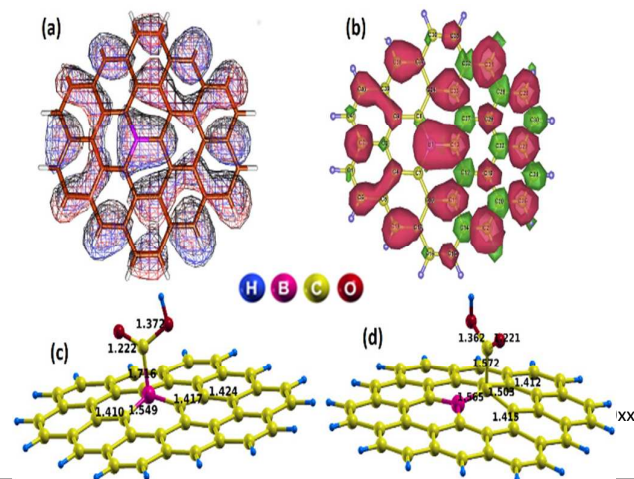


electrocatalytic CO<sub>2</sub> reduction against graphene.

Fig. 2 Linear sweep voltammetry of BG (dotted lines (b&c)) in 0.1 KHCO<sub>3</sub> in the presence (blue) and absence (red) of CO<sub>2</sub>. Dark solid trace (a) is the LSV of CO<sub>2</sub> reduction on graphene.

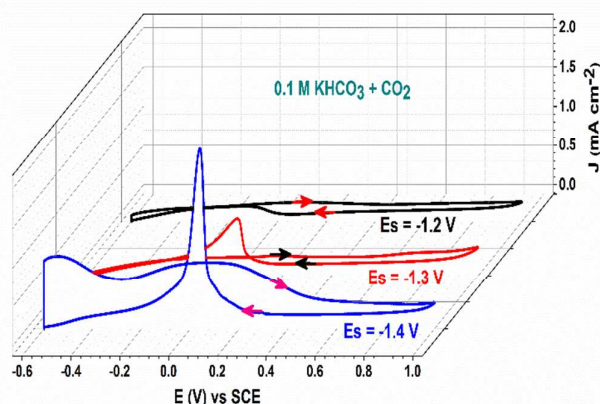
Fig. 3 a) HOMO of C<sub>41</sub>BH<sub>16</sub> (b) Spin density mapping (c) Chemisorption of \*COOH on C<sub>41</sub>BH<sub>16</sub> via B atom (d) Chemisorption of \*COOH on C<sub>41</sub>BH<sub>16</sub> via C atom.

For the preliminary product identification using substrate generation-tip collection mode (SG-TC) of scanning electrochemical microscopy (SECM).<sup>16</sup> It is advantageous that formate/formic acid, alcohols and CO, that are formed invariably found in the analysis of CO<sub>2</sub> reduction products are electroactive and hence amenable to detection in SECM. Since SECM can measure local chemical events at the interfaces, this technique offers the advantage of instantaneously sensing the (electroactive) species generated from the reaction taking place at the substrate.<sup>17</sup> In this mode of SECM, the substrate is poised at a fixed potential in the cathodic region and Pt UME tip voltammetry is recorded in the anodic potential regime.



The voltammetric response of the UME tip (in the tip-collection mode) to the product species generated at the substrate (in the SG-TC analysis) confirms the occurrence of electroreduction of CO<sub>2</sub>. Figure 4 shows the tip (Pt UME) response when the substrate (BG coated Glassy carbon electrode) is kept at different cathodic potentials at which the current (due to the anodic oxidation of the products of CO<sub>2</sub> reduction) starts increasing. Formate oxidation on the Pt tip can be identified when the substrate potential (E<sub>s</sub>) is kept at -1.2V with increasing currents at E<sub>s</sub> = -1.3V. This tip current becomes intense at E<sub>s</sub> = -1.4V indicating increased formation of formate ion at the substrate. Another important feature of the Pt tip response is noticeable when E<sub>s</sub> is kept at -1.4V. In addition to the intense formate oxidation peak, a new peak pair is observed between -0.6 and -0.4V that can be attributed to the oxidation of H<sub>2</sub> produced at the substrate.<sup>17</sup> That the reduction process leads solely to the formation of formate is conspicuous by the absence of CV signature responses of CO oxidation at the Pt UME probe. In a control experiment, we show the emergence of CO product during CO<sub>2</sub>RR on a gold surface, whose presence is indicated by the oxidative voltammetry of CO oxidation at Pt [ESI, Figure S4].

Fig. 4 (SG-TC Mode) Cyclic voltammetric response of Pt UME tip probe to the product(s) generated from B-doped graphene-modified substrate biased at different substrate potentials (E<sub>s</sub>) in 0.1M KHCO<sub>3</sub> saturated with CO<sub>2</sub>; Tip scan rate: 0.05Vs<sup>-1</sup>.



Mechanistically, formic acid formation from CO<sub>2</sub> reduction follows (2H<sup>+</sup> + 2e<sup>-</sup>) pathway<sup>18</sup> with the first step being CO<sub>2</sub> physisorption on the catalyst surface followed by chemisorption of the protonated CO<sub>2</sub> (\*COOH), equation (1). The next step is the attack of (H<sup>+</sup> + e<sup>-</sup>) on \*COOH to yield formic acid. The values of adsorption energy of CO<sub>2</sub> and \*COOH on graphene (C<sub>42</sub>H<sub>16</sub>) are found to be -0.61 and -1.50 kcalmol<sup>-1</sup> respectively. This suggests that the interaction of graphene with CO<sub>2</sub> and \*COOH is negligible and hence inconsequential. However for the first step on BG (C<sub>41</sub>BH<sub>16</sub>), it is observed that CO<sub>2</sub> physisorbs with an adsorption energy of -3.40 kcalmol<sup>-1</sup>. Further, for the chemisorption of the protonated CO<sub>2</sub> (i.e., \*COOH) on BG, there is a possibility that \*COOH can form a bond either via B or C atom of BG, as both B and C atoms possess spin densities (see

Figure 3(c-d)). Either way the chemisorption is feasible; which is reflected in higher adsorption energies. The adsorption energy of \*COOH on B and C in BG respectively is found to be -34.35 and -37.55 kcalmol<sup>-1</sup>. Second step (II reductive protonation) involves the formation of formic acid which proceeds on BG via equation 2; in this step of reduction, the chemisorbed \*COOH desorbs from the BG surface and yields formic acid as the major product with the regeneration of catalytically active sites. This is clear from the similar bond lengths of C-B and C-C in BG during the course of the reaction (Figure S8 (a) and S9 (P1)). In order to substantiate the selectivity of formic acid as a major product over CO on BG, we have calculated the relative energies of the reactants and products. (Detailed explanation given in ESI)

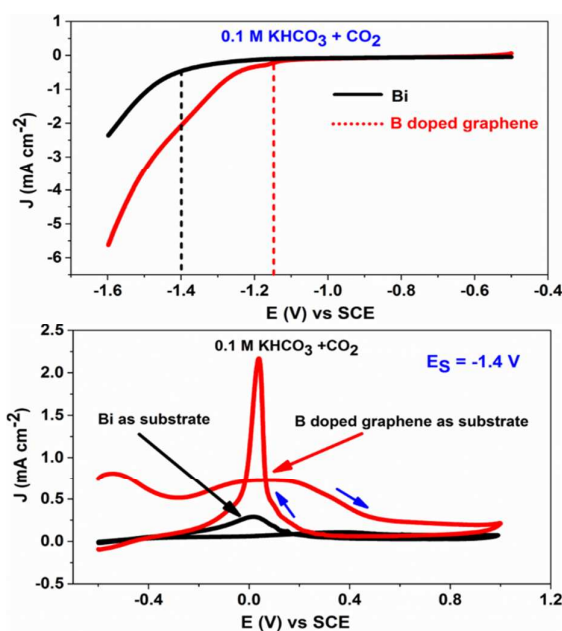
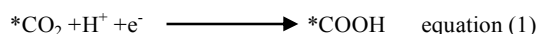


Fig. 5 (a), LSV of BG (red dotted line) and Bi (black solid line) in 0.1 KHCO<sub>3</sub> in the presence of CO<sub>2</sub> (b) SG-TC Mode: Cyclic voltammetric response of Pt UME tip probe to the product generated from the B doped graphene (red) and Bi (black) kept at a substrate potential (E<sub>s</sub>) -1.4V in 0.1 M KHCO<sub>3</sub> saturated with CO<sub>2</sub>; scan rate 0.05Vs<sup>-1</sup>.

In the next experiment, we compare the electrocatalytic activity of BG with a benchmark catalyst, Bi which selectively reduces CO<sub>2</sub> to formic acid.<sup>18</sup> LSV and SG-TC mode of SECM were used for the comparison of electrochemical activity. Figure 5(a) shows a comparison of the LSV of BG and Bi in CO<sub>2</sub>-saturated bicarbonate solutions. There is a 250 mV anodic shift in the onset potential of BG compared to Bi. Similarly in SECM, the tip current obtained during the oxidation of formate generated from the BG substrate is higher than that of Bi substrate. Constant potential electrolysis was carried out to check stability and for the product quantification (Figure S5).

$^1\text{H-NMR}$  analysis (Figure S6) was performed on the products of bulk electrolysis to calculate the faradaic efficiency (ESI). The faradaic efficiency of formate production on B-doped graphene at -1.4 V works out to be 66 % whereas for Bi it is 20 %. All these results suggest that B-doped graphene produces formate with a higher faradaic efficiency at overpotential lower than that of Bi. But the faradaic efficiency of Bi increases at higher cathodic potentials whereas it decreases in the case of B-doped graphene because of low hydrogen overpotential compared to that of Bi.

In summary, BG is shown to electrocatalyse the reduction of  $\text{CO}_2$  to formate. In bulk electrolysis experiments, we find this catalyst to remain stable without any significant degradation. It can thus be a model for the development of robust synthetic catalysts suitable for practical applications. DFT calculations show that boron-doping in graphene introduces asymmetric spin density, and making it suitable for electrocatalytic  $\text{CO}_2$  reduction by adsorbing on BG and not on pristine graphene and thereby undergo reduction to formate. We are currently examining boron-containing materials for their suitability to  $\text{CO}_2$  reduction and in some cases, the formation of CO is also encountered in both theory and experiment.

## Notes and references

- C. S. Chen, A. D. Handoko, J. H. Wan, L. Ma, and D. Ren, *Catal. Sci. Technol.*, 2015, **5**, 161–168
- (a) C. Costentin, M. Robert, and J.-M. Savéant, *Chem. Soc. Rev.*, 2013, **42**, 2423–2436; (b) W. Li, *ACS Symp. Ser.*, 2010, 55–76; (c) G. A. Olah, A. Goepfert, and G. K. S. Prakash, *J. Org. Chem.*, 2009, **74**, 487–498.
- E. E. Benson, C. P. Kubiak, A. J. Sathrum, and J. M. Smieja, *Chem. Soc. Rev.*, 2009, **38**, 89–99.
- X. Mao and T. A. Hatton, *Ind. Eng. Chem. Res.*, 2015, **54**, 4033–4042.
- R. Aydin, and F. Koleli, *Synth. Met.* 2004, **144**, 75–80.
- (a) E. B. Cole, P. S. Lakkaraju, D. M. Rampulla, A. J. Morris, E. Abelev, and A. B. Bocarsly, *J. Am. Chem. Soc.*, 2010, **132**, 11539–11551; (b) J. A. Keith and E. A. Carter, *Chem. Sci.*, 2013, **4**, 1490–1496.
- J. D. Froehlich, and C. P. Kubiak, *J. Am. Chem. Soc.* 2015, **137**, 4288–4291
- (a) S. Zhang, P. Kang, S. Ubnoske, M. K. Brennaman, N. Song, R. L. House, J. T. Glass, and T. J. Meyer, *J. Am. Chem. Soc.*, 2014, **136**, 7845–7848; (b) B. Kumar, M. Asadi, D. Pisasale, S. Sinha-Ray, B. A. Rosen, R. Haasch, J. Abiade, A. L. Yarin, and A. Salehi-Khojin, *Nat. Commun.*, 2013, **4**, 1–8; (c) J. Wu, R. M. Yadav, M. Liu, P. P. Sharma, C. S. Tiwary, L. Ma, X. Zhou, B. I. Yakobson, J. Lou, and P. M. Ajayan, *ACS Nano*, 2015, **9**, 5364–5371.
- (a) K. Gong, F. Du, Z. Xia, M. Durstock, and L. Dai, *Science*, 2009, **323**, 760–764; (b) R. Silva, D. Voiry, M. Chhowalla, and T. Asefa, *J. Am. Chem. Soc.*, 2013, **135**, 7823–7826;
- (a) Y. Zheng, Y. Jiao, L. Ge, M. Jaroniec, and S. Z. Qiao, *Angew. Chemie*, 2013, **125**, 3192–3198; (b) S. Wang, L. Zhang, Z. Xia, A. Roy, D. W. Chang, and J. Baek, L. Dai, *Angew. Chem. Int. Ed.*, 2012, **51**, 1–5.
- X. Wang, G. Sun, P. Routh, D. H. Kim, W. Huang, and P. Chen, *Chem. Soc. Rev.*, 2014, **43**, 7067–7098.
- (a) Q. Sun, Z. Li, D. J. Searles, Y. Chen, and A. Du, *J. Am. Chem. Soc.*, 2013, **135**, 8246–8253; (b) H. Choi, Y. C. Park, Y. Kim, and Y. S. Lee, *J. Am. Chem. Soc.*, 2011, **133**, 2084–2087.
- K. Nakata, T. Ozaki, C. Terashima, A. Fujishima, and Y. Einaga, *Angew. Chemie. Int. Ed.*, 2014, **53**, 871–874.
- (a) Z. H. Sheng, H. L. Gao, W. J. Bao, F. B. Wang, X. H. Xia, *J. Mater. Chem.* 2012, **22**, 390–395; (b) L. S. Panchakarla, K. S. Subrahmanyam, S. K. Saha, A. Govindaraj, H. R. Krishnamurthy, U. V. Waghmare, and C. N. R. Rao, *Adv. Mater.* 2009, **21**, 4726–4730.
- M. A. Nazrulla, S. Krishnamurthy, and K. L. N. Phani, *J. Phys. Chem. C*. 2014, **118**, 23058–23069.
- (a) C. M. Sanchez Sanchez, J. Rodriguez Lopez, and A. J. Bard, *Anal. Chem.*, 2008, **80**, 3254–3260; (b) P. Sun, O. Laforge and M. V. Mirkin, *Phys. Chem. Chem. Phys.* 2007, **9**, 802–823.
- N. Sreekanth and K. L. Phani, *Chem. Commun*, 2014, **50**, 11143–11146.
- Y. Hori, in *Modern Aspects of Electrochemistry 42* (eds C. G. Vayenas, R. E. White & M. E. Gamboa-Aldeco), Springer, 2008, 89–189.